AIP Physics of Fluids

Laboratory evidence of freak waves provoked by non-uniform bathymetry

K. Trulsen, H. Zeng, and O. Gramstad

Citation: Phys. Fluids **24**, 097101 (2012); doi: 10.1063/1.4748346
View online: http://dx.doi.org/10.1063/1.4748346
View Table of Contents: http://pof.aip.org/resource/1/PHFLE6/v24/i9
Published by the American Institute of Physics.

Laboratory evidence of freak waves provoked by non-uniform bathymetry

K. Trulsen,[a] H. Zeng,[b] and O. Gramstad[c]
Department of Mathematics, University of Oslo, Norway

(Received 14 July 2011; accepted 23 July 2012; published online 5 September 2012)

We show experimental evidence that as relatively long unidirectional waves propagate over a sloping bottom, from a deeper to a shallower domain, there can be a local maximum of kurtosis and skewness close to the shallower side of the slope. We also show evidence that the probability of large wave envelope has a local maximum near the shallower side of the slope. We therefore anticipate that the probability of freak waves can have a local maximum near the shallower side of a slope for relatively long unidirectional waves. © *2012 American Institute of Physics*. [http://dx.doi.org/10.1063/1.4748346]

I. INTRODUCTION

It is well known that as waves propagate from deeper to shallower water, linear refraction can transform the waves such that the wavelength becomes shorter, while the amplitude and the steepness become larger.[1,2]

We here address the question if the change of depth can provoke increased likelihood of freak waves. A freak wave satisfies a requirement that it is much more extreme than a typical "reference" wave, common criteria are $\eta_c/H_s > 1.25$ or $H/H_s > 2$ where the crest elevation is η_c and the wave height is H. Here the significant wave height H_s, defined as four times the standard deviation of the surface elevation, is used as reference.[3]

In an inhomogeneous medium we insist that it is most useful to avoid averaging over space for the determination of the reference wave, thus the significant wave height should be treated as a function of space and the criteria for freak waves become local.[4] While linear refraction transforms the local significant wave height, it is not anticipated that linear refraction itself can transform the probability of freak waves over changing bathymetry as long as the local criteria for freak waves suggested above are employed. This is indeed supported by our own recent numerical studies.[5]

On sufficiently deep water, long-crested waves are subject to modulational instability[6] which is known to spawn wave evolution that can lead to freak waves.[7–9] Nonlinear wave evolution of long-crested waves on deep water and the concomitant development of freak waves has been well described both theoretically[10–12] and experimentally.[13–19] One particular aspect that we shall be concerned with, is that nonlinear modulations during the evolution of irregular waves can cause spectral development and frequency down-shift, suspected to be related to the occurrence of freak waves.[12,15]

On flat bottom of finite depth h, various competing processes determine the nonlinear wave evolution. The modulational instability becomes weaker as the depth is decreased,[20] and vanishes altogether for uniform long-crested waves on small depths $kh < 1.363$ where k is the wavenumber corresponding to the depth h.[21] On the other hand, if the steepness increases due to linear refraction, as discussed above, the effect of modulational instability could be enhanced, at least when $kh > 1.363$. Limiting to flat bottom, these nonlinear properties are contained within the Zakharov equation.[22]

[a]Author to whom correspondence should be addressed. Electronic mail: karstent@math.uio.no.
[b]Electronic mail: huimingz@math.uio.no.
[c]Electronic mail: oding@math.uio.no.

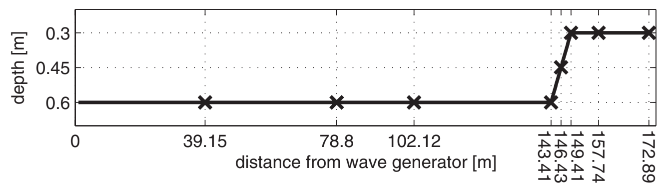

FIG. 1. The bottom profile and locations of the wave probes.

While the modulational instability is attenuated for decreasing depth, static nonlinearities such as second-order effects are enhanced, but even so Janssen[23] anticipated that the final outcome could still be that the kurtosis decreases for diminishing depth of a flat bottom.

On variable depth, the variation of kurtosis of nonlinear waves has been computed in some recent numerical studies. Janssen and Herbers[24] studied the kurtosis of initially long-crested waves, becoming directional as they refracted over a submerged shoal in otherwise deep water. They found that strongly non-Gaussian behavior can be produced due to the concomitant effects of focusing and nonlinearity. The maximum kurtosis was found down-wave of the location of the steepest waves near the top of the shoal. Their deeper kh was around 20 and their shallower kh was 0.22. Sergeeva, Pelinovsky, and Talipova[25] employed a KdV equation for variable depth for long-crested waves propagating over a slope connecting two domains of different constant depth. They found that the kurtosis could achieve a local maximum close to the shallower side of the slope. In their case the deeper kh was 0.44 and the shallower kh was 0.3 and the gradient of the depth was 0.03. Zeng and

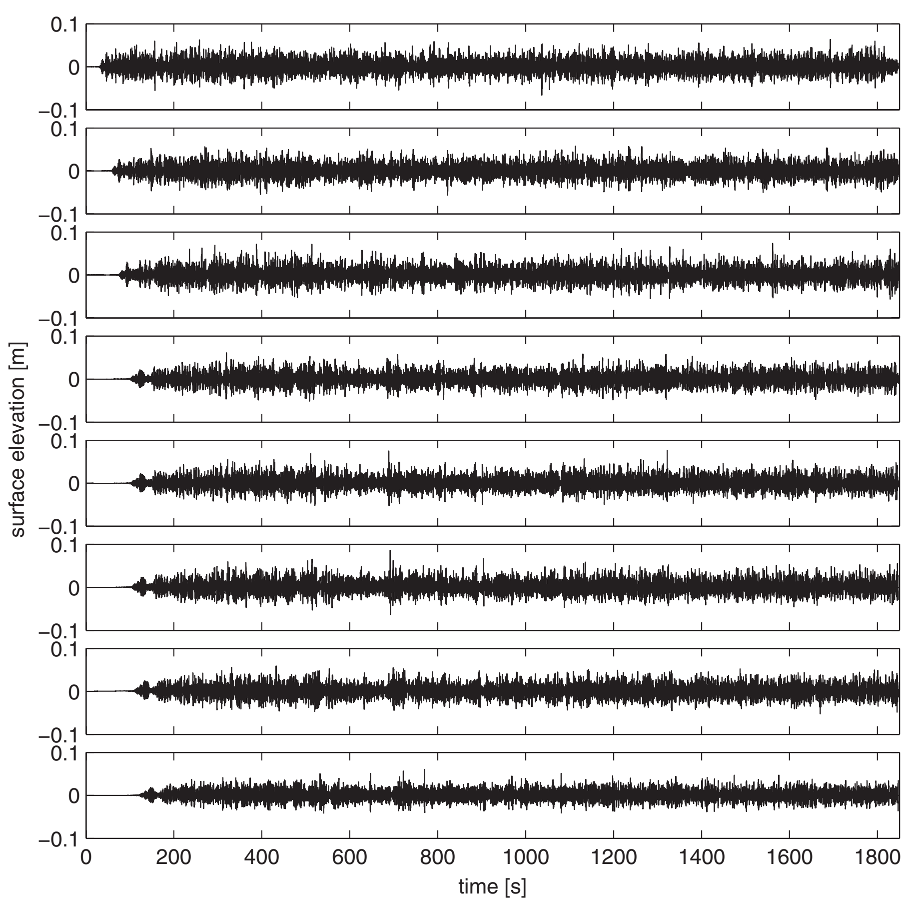

FIG. 2. Time series for all probes for case 1.

TABLE I. Three cases.

Case	H_s [m]	T_p [s]	Deeper side k_ph	Deeper side k_pa_c	Deeper side Ur	Shallower side k_ph	Shallower side k_pa_c	Shallower side Ur
1	0.06	1.273	1.6	0.057	0.014	0.99	0.070	0.072
2	0.06	1.697	1.1	0.038	0.029	0.70	0.049	0.14
3	0.06	2.121	0.81	0.028	0.053	0.54	0.038	0.24

Trulsen[5] used a nonlinear Schrödinger (NLS) equation for variable depth to investigate long-crested waves propagating over a slope connecting two domains of different constant depth, with the deeper kh being 10 and the shallower kh being between 1.2 and 4.0. With our shallower domain being much deeper than those of the other authors,[24,25] we found that the kurtosis could be significantly reduced toward the shallower domain, and a local minimum of kurtosis could be achieved near the shallower

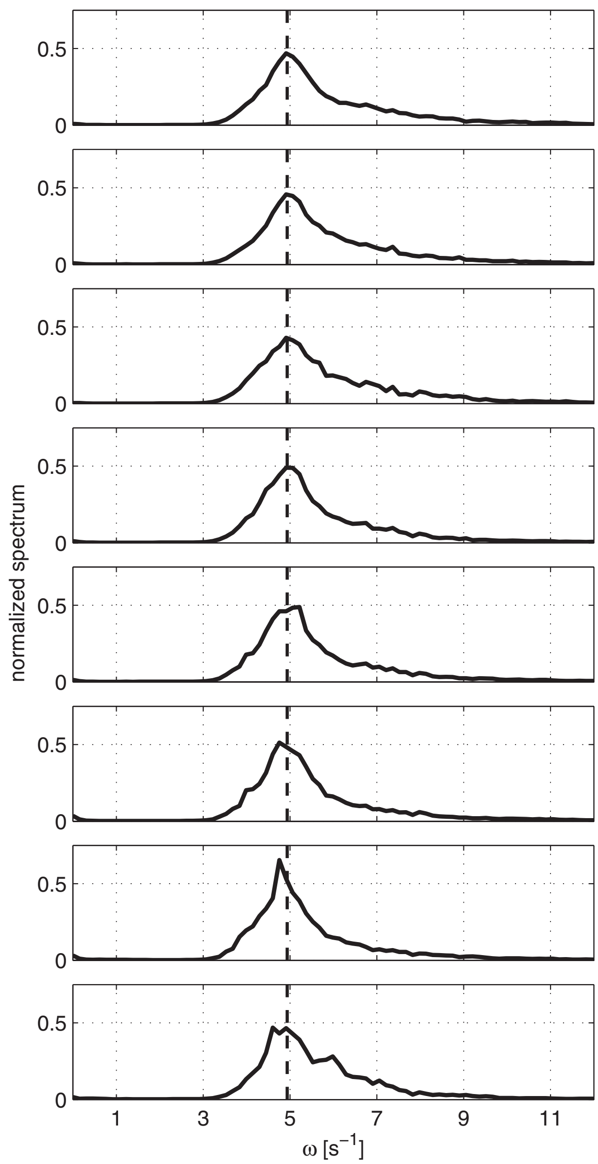

FIG. 3. Normalized frequency spectrum $S(\omega)$ for all probes for case 1 with linear scales. Nominal peak frequency indicated by vertical dashed line.

side of the slope. We therefore speculate that there may exist a transition zone between two opposite regimes, a "deeper" regime with reduction of kurtosis toward the shallower side, and a "shallower" regime with a possible maximum of kurtosis near the shallower side.

We are not aware of previous analysis of laboratory experiments discussing the statistical behavior suggested by the above three papers.[5,24,25] While there are available analysis of field measurements of waves on a sloping bottom near a coast,[26–28] we hesitate to apply those for our present purposes since both short-crestedness and skew incidence may have important effects so far not accounted for in the numerical modeling.

The present paper provides experimental evidence of the above numerical predictions for long-crested waves propagating normally incident over non-uniform bathymetry. Such evidence was found in experiments recently carried out at Marin in The Netherlands.[29] We show that as the waves propagated over a slope, from a deeper to a shallower domain, there was a local maximum of kurtosis and skewness near the shallower side of the slope, accompanied by a local increased probability of

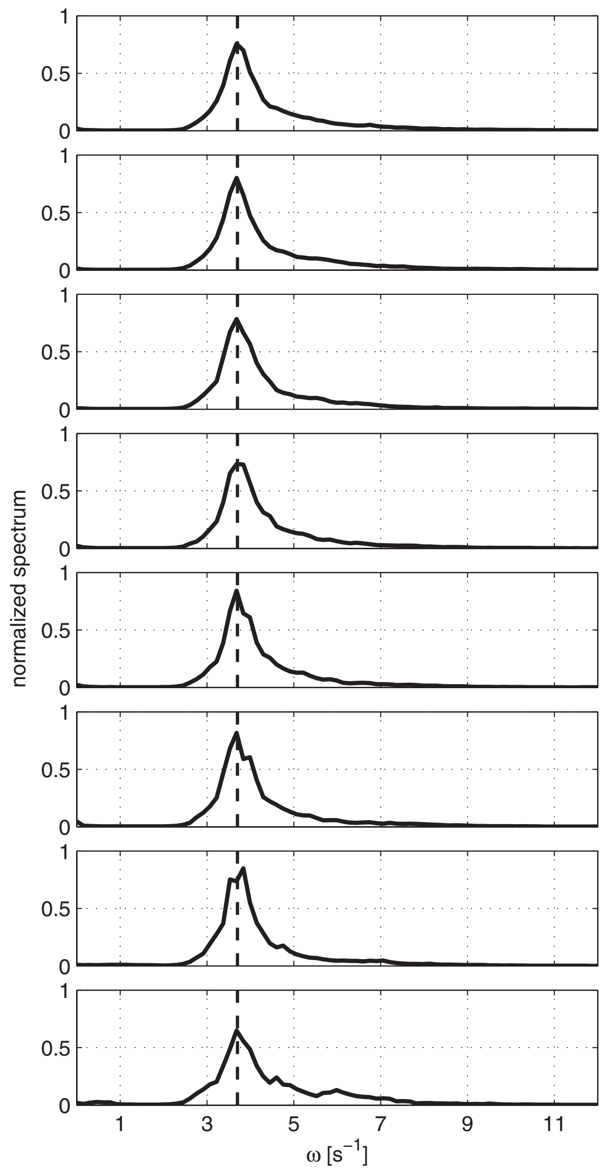

FIG. 4. Same as Fig. 3 for case 2.

large envelope height. It will be realized that the range of shallower *kh* of the experiments does not coincide with any of the three numerical studies,[5,24,25] but falls within the suspected transition zone between the "deeper" and "shallower" regime.

II. EXPERIMENT

The experiments were performed at Marin in The Netherlands for a benchmark workshop on numerical wave modeling.[29] Irregular long-crested waves were propagated over a 1:20 slope from water of constant depth 0.60 m to water of constant depth 0.30 m. Between the wave generator and the start of the slope, the bottom was flat with depth 0.60 m. The distance from the wave generator to the start of the slope was 143.41 m. The slope ended at 149.41 m from the wave generator. Behind the slope there was a flat bottom with depth 0.30 m. A beach started at 173.41 m from the wave generator. The wave probes were located at distances 39.15 m, 78.80 m, 102.12 m, 143.41 m,

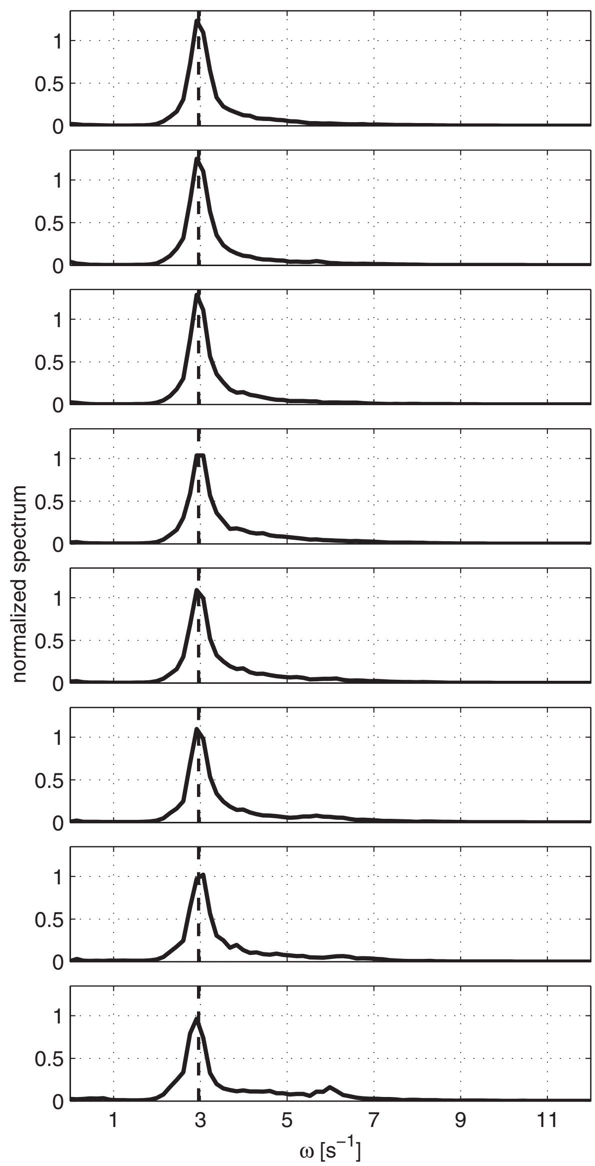

FIG. 5. Same as Fig. 3 for case 3.

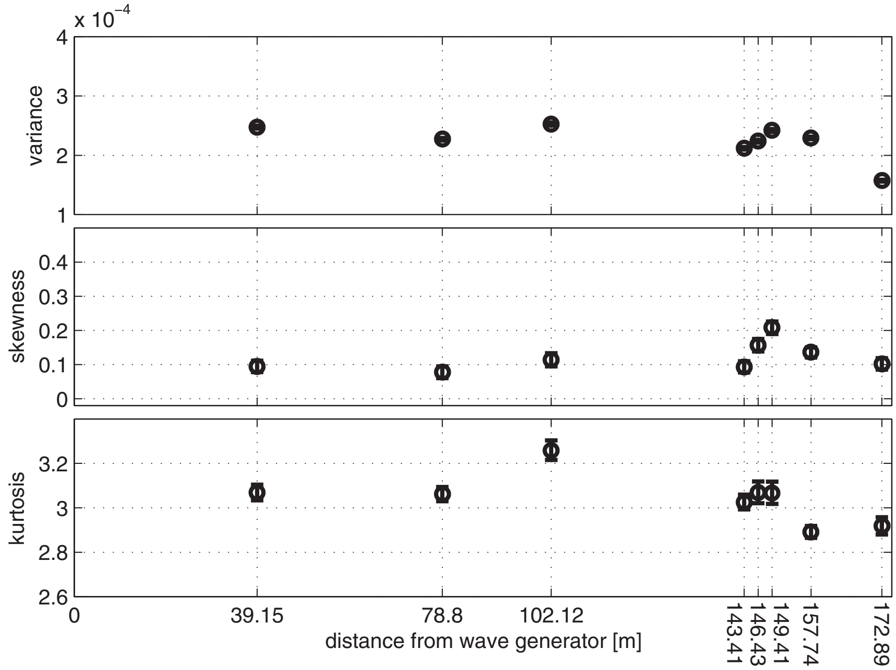

FIG. 6. Statistics for case 1.

146.43 m, 149.41 m, 157.74 m, and 172.89 m from the wave generator. The bottom profile and the locations of the wave probes are shown in Fig. 1.

Three cases of long-crested irregular waves were employed, generated with constant nominal significant wave height H_s and different nominal peak periods T_p, as shown in Table I. The peak wavenumber k_p has been computed from the linear dispersion relation $\omega_p^2 = g k_p \tanh k_p h$ where

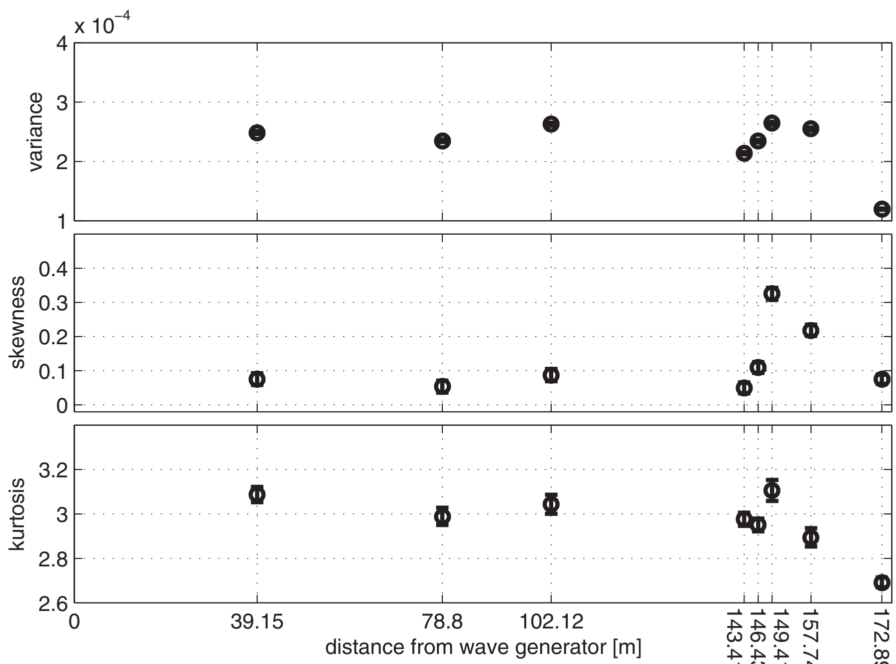

FIG. 7. Statistics for case 2.

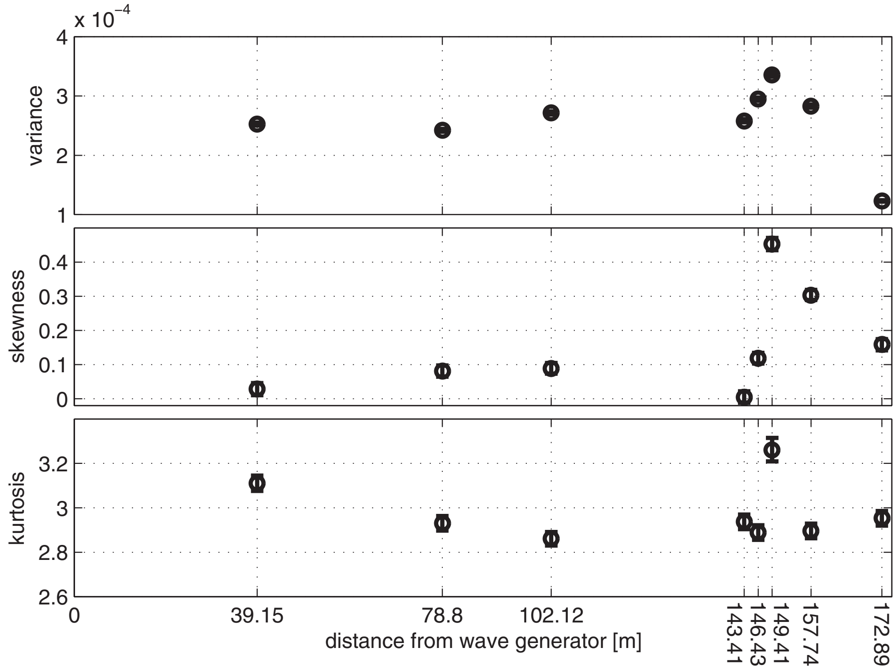

FIG. 8. Statistics for case 3.

$\omega_p = 2\pi/T_p$ using the acceleration of gravity $g = 9.81$ m^2/s. We have defined the characteristic amplitude $a_c = H_s/\sqrt{8}$ corresponding to a uniform wave of the same mean power. The Ursell number has been computed as $Ur = k_p a_c/(k_p h)^3$. We remark that Cherneva *et al.*[26] employed a parameter $\omega_h = \omega_p\sqrt{h/g}$ as an alternative to our $k_p h$, they are related by $\omega_h^2 = k_p h \tanh k_p h$.

For the three cases the time series have, respectively, 92 378, 91 969 and 92 148 time samples taken with uniform interval $\Delta t = 0.02$ s. The time series of case 1 are shown in Fig. 2 suggesting some startup effects. The first 10 000 samples (200 s) are not included in the subsequent analysis in order to exclude the startup effects. This leaves us with some 1294, 966, and 774 peak periods for each case, respectively. These are rather insufficient amounts to achieve meaningful freak wave statistics according to common criteria such as $\eta_c/H_s > 1.25$ or $H/H_s > 2$,[3] but sufficient for reasonable estimates of kurtosis, skewness and overall distribution functions.

The spectra at each probe for cases 1, 2, and 3 are shown in Figs. 3–5 with linear scales. The vertical dashed lines show the nominal peak frequencies ω_p, and help illustrate that there is spectral development leading to a downshift of the peak clearly visible in case 1, but not in the other two cases. Indeed, from Table I we anticipate modulational instability only for the deeper side of case 1. The bandwidths can be estimated by inspection of Figs. 3–5. The ratio between the half-peak half-width and the peak frequency is estimated to be approximately 0.1 in all cases for the probe closest to the wave maker.

In Figs. 6–8 we show the variance of the surface elevation in the upper frame, the skewness of the surface elevation in the middle frame and the kurtosis of the surface elevation in the lower frame. For the three statistical estimates we also indicate 95% confidence intervals obtained from 10 000 bootstrap samples from the original dataset.

For all three cases there is a local maximum of variance, skewness, and kurtosis at or near the shallower edge of the slope.

For case 1, Fig. 6, the global maximum of the kurtosis happens within the domain of deeper constant depth. This is likely related to the spectral evolution leading to a downshift of the spectral peak seen in Fig. 3, and is also likely related to the fact that the deeper kh is greater than 1.363 as seen in Table I. For this case, the smaller local maximum of kurtosis and the global maximum of skewness at the shallower edge of the bottom slope are most likely not due to modulational instability since here the depth is smaller than the threshold value.

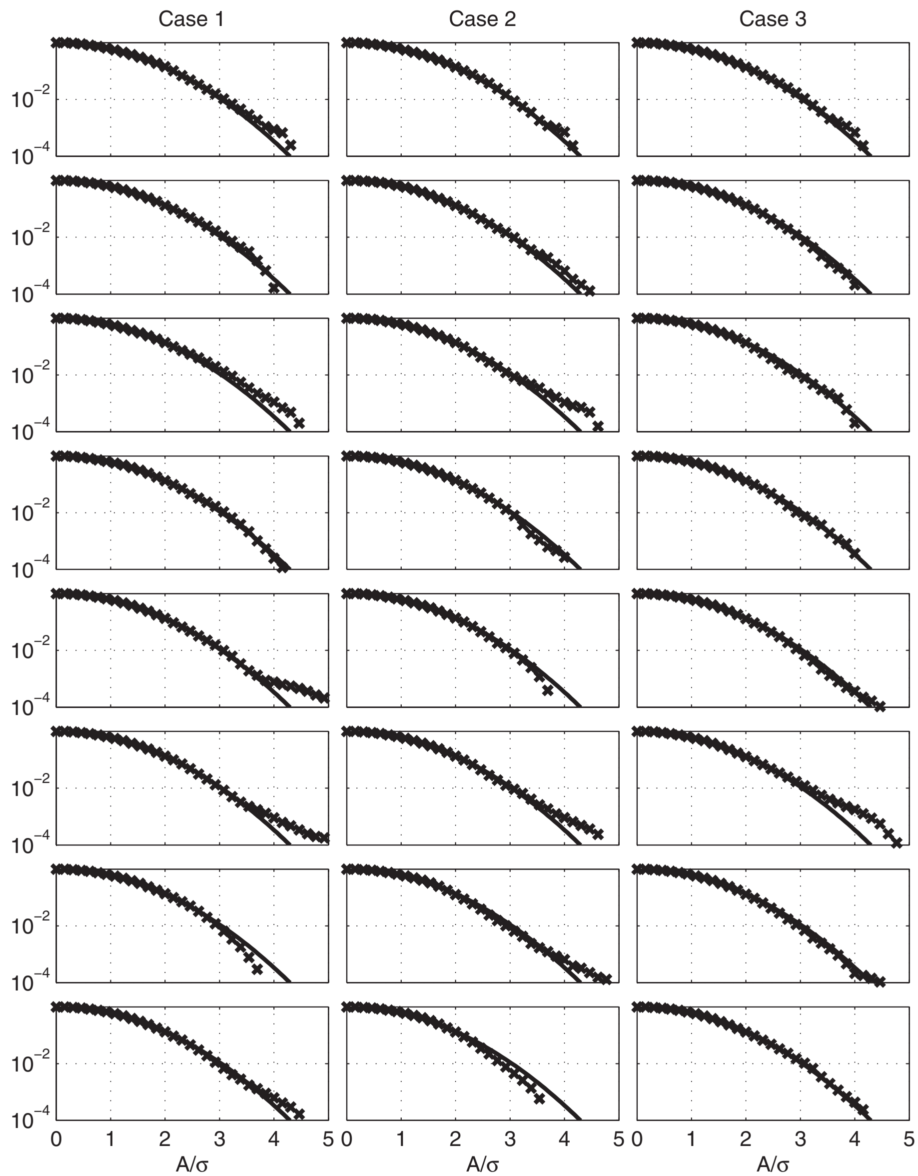

FIG. 9. Exceedance function of the wave envelope A normalized by the standard deviation σ of the surface elevation at each individual location (crosses), compared to the exceedance function of the Rayleigh distribution (solid line). The rows from top to bottom correspond to the eight wave probes, from left to right in Fig. 1, respectively. The columns from left to right correspond to the three cases 1, 2 and 3.

For cases 2 and 3, Figs. 7 and 8, there is a global maximum of all three statistical quantities at the shallower edge of the slope. In both of these cases, the depth is everywhere smaller than the threshold value for modulational instability, and no shift of the spectral peak can be easily seen in Figs. 4 and 5. For these cases, the global maximum of kurtosis coincides with the global maximum of the variability of the kurtosis estimate.

In Fig. 9 we show the exceedance probability of the wave envelope, $1 - P$, where P is the cumulative distribution function of the wave envelope, and compare with the Rayleigh distribution, at the various measurement stations. The envelope $A(t)$ was obtained by taking the Hilbert transform $\tilde{\eta}(t)$ of the surface elevation $\eta(t)$ and computing $A(t) = \sqrt{\{\tilde{\eta}(t)\}^2 + \{\eta(t)\}^2}$, see Ochi.[30] In the figure the envelope has been normalized by the standard deviation of the surface elevation appropriate for each individual measurement station. We interpret deviation from the Rayleigh distribution as an indication of non-Gaussian behavior of the surface elevation beyond static second-order effects. The only location where all cases yield a systematic increase in extreme wave occurrence beyond Gaussian statistics is at the sixth probe located at the shallow edge of the slope. There is also evidence of increased extreme wave probability at the third probe on top of the deeper domain, likely related to nonlinear modulational effects for the two deeper cases 1 and 2.

There is available field experimental evidence of significantly enhanced freak wave occurrence for sloping bottom, e.g., Fig. 11(c) in Cherneva *et al.*[26] for even smaller depth than considered here (their $\omega_h = 0.4738$, our smallest $\omega_h = 0.518$), but it is not clear that such comparison can be justified due to unknown details of direction of wave incidence and directional spectrum.

III. CONCLUSIONS

We have shown experimental evidence that as long-crested waves propagate normally incident over a sloping bottom, from a deeper to a shallower domain, there can be a local maximum of kurtosis and skewness close to the shallower side of the slope, and there can be a local maximum of probability of large wave envelope at the same location. We therefore anticipate a corresponding local maximum of freak wave probability here as well.

ACKNOWLEDGMENTS

We thank Janou Hennig, Tim Bunnik, and Christian Schmittner at Marin in The Netherlands for making the dataset available, and the referees for constructive remarks. This research has been supported by the Research Council of Norway through Grant No. 177464/V30.

[1] C. C. Mei, *The Applied Dynamics of Ocean Surface Waves* (World Scientific, 1989), 740 pp.
[2] Y. Goda, *Random Seas and Design of Maritime Structures* (World Scientific, 2000).
[3] K. Dysthe, H. E. Krogstad, and P. Müller, "Oceanic rogue waves," Annu. Rev. Fluid Mech. **40**, 287–310 (2008).
[4] K. B. Hjelmervik and K. Trulsen, "Freak wave statistics on collinear currents," J. Fluid Mech. **637**, 267–284 (2009).
[5] H. Zeng and K. Trulsen, "Evolution of skewness and kurtosis of weakly nonlinear unidirectional waves over a sloping bottom," Nat. Hazards Earth Syst. Sci. **12**, 631–638 (2012).
[6] T. B. Benjamin and J. E. Feir, "The disintegration of wave trains on deep water," J. Fluid Mech. **27**, 417–430 (1967).
[7] E. A. Kuznetsov, "Solitons in a parametrically unstable plasma," Sov. Phys. Dokl. **22**, 507–508 (1977).
[8] T. Kawata and H. Inoue, "Inverse scattering method for the nonlinear evolution equations under nonvanishing conditions," J. Phys. Soc. Jpn. **44**, 1722–1729 (1978).
[9] K. B. Dysthe and K. Trulsen, "Note on breather type solutions of the NLS as models for freak-waves," Phys. Scr. **T82**, 48–52 (1999).
[10] M. Onorato, A. R. Osborne, M. Serio, and S. Bertone, "Freak waves in random oceanic sea states," Phys. Rev. Lett. **86**, 5831–5834 (2001).
[11] M. Onorato, A. Osborne, R. Fedele, and M. Serio, "Landau damping and coherent structures in narrow-banded 1+1 deep water gravity waves," Phys. Rev. E **67**, 1–6 (2003).
[12] H. Socquet-Juglard, K. Dysthe, K. Trulsen, H. E. Krogstad, and J. Liu, "Probability distributions of surface gravity waves during spectral changes," J. Fluid Mech. **542**, 195–216 (2005).
[13] M. Onorato, A. R. Osborne, M. Serio, L. Cavaleri, C. Brandini, and C. T. Stansberg, "Observation of strongly non-Gaussian statistics for random sea surface gravity waves in wave flume experiments," Phys. Rev. E **70**, 1–4 (2004).
[14] M. Onorato, A. R. Osborne, and M. Serio, "Modulational instability and non-Gaussian statistics in experimental random water-wave trains," Phys. Fluids **17**, 1–4 (2005).
[15] M. Onorato, A. R. Osborne, M. Serio, L. Cavaleri, C. Brandini, and C. T. Stansberg, "Extreme waves, modulational instability and second order theory: wave flume experiments on irregular waves," Eur. J. Mech. B/Fluids **25**, 586–601 (2006).
[16] P. Petrova and C. Guedes Soares, "Maximum wave crest and height statistics of irregular and abnormal waves in an offshore basin," Appl. Ocean Res. **30**, 144–152 (2008).
[17] Z. Cherneva, M. A. Tayfun, and C. Guedes Soares, "Statistics of nonlinear waves generated in an offshore wave basin," J. Geophys. Res. **114**, C08005, doi:10.1029/2009JC005332 (2009).
[18] F. Fedele, Z. Cherneva, M. A. Tayfun, and C. Guedes Soares, "Nonlinear Schrödinger invariants and wave statistics," Phys. Fluids **22**, 036601 (2010).
[19] Z. Cherneva and C. Guedes Soares, "Evolution of wave properties during propagation in a ship towing tank and an offshore basin," Ocean Eng. **38**, 2254–2261 (2011).
[20] D. J. Benney and G. J. Roskes, "Wave instabilities," Stud. Appl. Math. **48**, 377–385 (1969).
[21] G. B. Whitham, "Variational methods and applications to water waves," Proc. R. Soc. London **299**, 6–25 (1967).
[22] P. A. E. M. Janssen and M. Onorato, "The intermediate water depth limit of the Zakharov equation and consequences for wave prediction," J. Phys. Oceanogr. **37**, 2389–2400 (2007).

[23] P. A. E. M. Janssen, "On some consequences of the canonical transformation in the Hamiltonian theory of water waves," J. Fluid Mech. **637**, 1–44 (2009).
[24] T. T. Janssen and T. H. C. Herbers, "Nonlinear wave statistics in a focal zone," J. Phys. Oceanogr. **39**, 1948–1964 (2009).
[25] A. Sergeeva, E. Pelinovsky, and T. Talipova, "Nonlinear random wave field in shallow water: variable Korteweg–de Vries framework," Nat. Hazards Earth Syst. Sci. **11**, 323–330 (2011).
[26] Z. Cherneva, P. Petrova, N. Andreeva, and C. Guedes Soares, "Probability distributions of peaks, troughs and heights of wind waves measured in the Black Sea coastal zone," Coastal Eng. **52**, 599–615 (2005).
[27] I. Didenkulova and C. Anderson, "Freak waves of different types in the coastal zone of the Baltic Sea," Nat. Hazards Earth Syst. Sci. **1**, 2021–2029 (2010).
[28] I. Didenkulova, "Shapes of freak waves in the coastal zone of the Baltic Sea (Tallinn Bay)," Boreal Environment Research **16**(A), 138–148 (2011).
[29] T. Bunnik, "Benchmark workshop on numerical wave modeling — description of test cases," Technical Report 70022–1–RD (MARIN, The Netherlands, 2010).
[30] M. K. Ochi, *Ocean Waves* (Cambridge, 1998).